The LINNEAN SOCIETY of London ZOOLOGICAL Journal of the Linnean Society

Zoological Journal of the Linnean Society, 2015, **174**, 447–458. With 4 figures

Geographical distribution and evolutionary divergence times of Asian populations of the brine shrimp *Artemia* (Crustacea, Anostraca)

AMIN EIMANIFAR[1]*, GILBERT VAN STAPPEN[2] and MICHAEL WINK[1]

[1]*Institute of Pharmacy and Molecular Biotechnology, Heidelberg University, Im Neuenheimer Feld 364, 69120 Heidelberg, Germany*
[2]*Laboratory of Aquaculture & Artemia Reference Center, Ghent University, Ghent, Belgium*

Received 28 July 2014; revised 28 December 2014; accepted for publication 29 December 2014

The brine shrimp *Artemia* represents a widespread genus of microcrustaceans adapted to hypersaline environments. The species of this genus have been the subject of numerous phylogenetic studies, but many open questions remain, especially for Eurasian *Artemia* lineages. *Artemia sinica* Cai, 1989 and *Artemia tibetiana* have a restricted geographical distribution, whereas the Eurasian haplotype complex (EHC) and especially *Artemia urmiana* Günther, 1899 show wider ranges. We examined the geographic distribution, evolutionary age, and historical demography of the Asian *Artemia* lineages (*A. urmiana*, *A. sinica*, *A. tibetiana*, and the Eurasian haplotype complex) using samples from 39 geographical localities and based on the nucleotide sequences of the mitochondrial cytochrome *c* oxidase subunit I (*COI*) gene. Asian *Artemia* taxa clusters into four distinctive clades with high nodal support, consisting of 69 unique haplotypes. A star-like haplotype pattern was visible in EHC lineages (comprising pathenogenetic populations), which were genetically close to two sexual species, *A. urmiana* and *A. tibetiana*. The Bayesian approach of molecular clock estimation indicated that *A. sinica* had already diverged in the late Miocene (19.99 Mya), whereas *A. urmiana*, *A. tibetiana*, and EHC shared a common ancestor in the late Pliocene (5.41 Mya). Neutrality tests indicated a recent population expansion in *A. urmiana* and EHC lineages. The diversification within *A. urmiana* and EHC lineages occurred in the Pleistocene (1.72 Mya) and Holocene (0.84 Mya), respectively. Overall, these results suggest a much longer evolutionary history of *A. sinica* and the possible evolutionary origin of EHC lineages from Asian sexual ancestors. Our findings point to the importance of species structure and divergence time variations of Asian *Artemia*, highlighting interspecific diversification and range expansion of local species in Asia.

doi: 10.1111/zoj.12242

ADDITIONAL KEYWORDS: Asian *Artemia* – *COI* marker – evolutionary age – geographic structure – mtDNA.

INTRODUCTION

Brine shrimps *Artemia* (Crustacea, Anostraca) are cosmopolitan extremophile microcrustaceans distributed over 600 geographically isolated areas across the world, excepting Antarctica (Abatzopoulos *et al*., 2002). *Artemia* is the most successful survivor in hypersaline environments, with some populations reproducing sexually and others obligately asexually (parthenogenetically) (Gajardo & Beardmore, 2012).

Species circumscription in *Artemia* is strongly influenced by DNA sequence data and geographical distribution, because only a few distinctive morphological characters exist in this microcrustacean. Three sexual species are found in Asia: *Artemia urmiana* Günther, 1899 (Lake Urmia, Ukraine), *Artemia tibetiana* Abatzopoulos, Zhang & Sorgeloos, 1998 (Tibetan Plateau), and *Artemia sinica* Cai, 1989 (China and Mongolia); *Artemia* sp. from Kazakhstan (Pilla & Beardmore, 1994) is not taken into consideration here, as its exact

*Corresponding author. E-mail: amineimanifar@yahoo.com; A.Eimanifar@uni-heidelberg.de

geographical origin is unknown. Abatzopoulos *et al*. (2002) suggested that parthenogenetic *Artemia* populations cannot readily be considered as belonging to the single species *Artemia parthenogenetica* Barigozzi, 1974, and therefore proposed 'parthenogenetic populations' or 'parthenogenetic strains' as an alternative without taxonomic consequences.

In general we only have information on the origin of samples, and we have not checked their reproductive modes under laboratory conditions; therefore, we have now introduced the term Eurasian haplotype complex (EHC) to describe a large group of putative parthenogenetic *Artemia* populations sharing the same haplotype complex, which includes documented parthenogenetic populations. According to DNA analysis EHC lineages are widely distributed over Eurasia, extending from the Canary Islands to China (Maccari, Amat & Gómez, 2013; Eimanifar *et al*., 2014).

The evolutionary history and population structure of European, African, and Asian parthenogenetic populations have been investigated based on nucleotide sequences from mitochondrial and nuclear DNA (mtDNA and ncDNA; Baxevanis, Kappas & Abatzopoulos, 2006; Muñoz *et al*., 2010; Maccari *et al*., 2013). Some Eurasian parthenogenetic populations have probably been generated through hybridization between closely related Asian species, and additionally through the contagious parthenogenesis mechanism upon the occurrence of rare males within parthenogenetic populations (Maccari *et al*., 2013, 2014; Xu *et al*., 2013).

Divergence times of Asian *Artemia* lineages have partially been determined (Baxevanis *et al*., 2006), but a more comprehensive phylogeny and evolutionary history of Asian lineages would be useful to understand the evolution and adaptation of brine shrimp lineages in Asia. Therefore, the purpose of the present study is to further evaluate the phylogeography of Asian lineages. We used the mitochondrial cytochrome *c* oxidase subunit I (*COI*) gene (commonly employed by authors working on brine shrimps) to form a better understanding of the geographic structure of Asian *Artemia*. The evolutionary age and divergence times of Asian *Artemia* were estimated based on a maximum-parsimony molecular clock approach.

MATERIAL AND METHODS

Sampling collection and DNA extraction

We obtained 243 *Artemia* samples collected from 39 geographical localities throughout Asia. All samples were collected by us or originated from the cyst bank of the Laboratory of Aquaculture & *Artemia* Reference Centre (ARC), Ghent University, Belgium. A full list of *Artemia* samples, Institute of Pharmacy and Molecular Biotechnology (IPMB) voucher numbers, species status, and GPS coordinates of all localities are shown in Table 1. Additional sequences from GenBank were included in our data set, as shown in Table S1. Total genomic DNA was isolated from individual cysts of *Artemia* using a Chelex-based method, followed by proteinase K digestion at 56 °C for 2 h (Eimanifar & Wink, 2013). Extracted DNA was stored at –20 °C, and used for further genetic analysis.

Polymerase chain reaction (PCR) amplification and sequencing

A fragment of *COI* was amplified via PCR in a total volume of 50 µl, containing 2 µl of template DNA, 2 µL of deoxynucleotide triphosphates (dNTPs; 1.25 mM), 5 µL 10× *Taq* buffer, 1 µL each primer (10 µM), 38.8 µL distilled water, and 0.2 µL *Taq* DNA polymerase (5 U μl^{-1}; Bioron, Ludwigshafen, Germany). The primer sequence used in the present study was *COI*_F (5′-ATTCTACGAATCACAAGGATATTGG-3′) and *COI*_R (5′-TACACTTCAGGATGGCCAAAAAATCA-3′). Cycling profile for PCR amplifications was 5 min at 94 °C (one cycle), 50 s at 94 °C, 1 min at 53 °C, and 60 s at 72 °C (36 cycles), followed by a final extension of 7 min at 72 °C. Amplified PCR products (710 base pairs) were visualized by electrophoresis on a 1% agarose gel stained with Ethidium Bromide (Serva Co.). All PCR products were purified according to the method described by Eimanifar & Wink (2013). The purified products were directly sequenced in two reactions with the same primer used in PCR amplification as described by Eimanifar & Wink (2013).

All sequences were aligned automatically using BIOEDIT 7.1.3.0 (Hall, 1999). In order to make sure that base calls were true at all polymorphic positions, we double-checked the whole data set against the original chromatogram. The aligned sequences were converted into amino acids using MEGA 6 in order to find a possible signal of nuclear pseudogenes (Tamura *et al*., 2013). An additional 277 *COI* sequences were retrieved from GenBank and added to our data set. In total, the data set included 520 *COI* sequences. The phylogenetic analyses were rooted using *Daphnia tenebrosa* (HQ972028) as the out-group.

Phylogenetic analysis

Phylogenetic analyses were carried out using maximum likelihood (ML) and Bayesian inference (BI). The best-fitting nucleotide substitution model based on Akaike's information criterion (AIC) was chosen using jModelTest 0.1.1 (Posada, 2008) for the reconstruction of ML and BI trees. The best-fitting model for the entire data set was TrN + I + G with the following parameters $-\ln L = 2514.30$ (A = 0.24, C = 0.23, G = 0.18,

Table 1. Origin of *Artemia* samples from Asia and Africa

No.	IPMB voucher/ ARC code number	Abbreviation for locality	Sample size	Species *A	Species *B	Locality, province, state, or district	Country	Geographic coordinates	GenBank accession numbers
1	64745/1206	XIE	9	S	S	Xiechi Lake, Shanxi	China	111°55′E, 35°44′N	KF691269–KF691277
2	66311	YUN	5	S	S	Yuncheng, Shanxi	China	110°58′E, 34°59′N	KF691298–KF691302
3	65829/1524	JIN	4	T	T	Jingyu Lake, Xinjiang	China	89°09′E, 36°03′N	KF691215–KF691218
4	57250	TIB1	5	T	T	Tibet	China	30°46′N, 85°48′E	KF691245–KF691249
5	57248	TIB2	3	T	T	Tibet	China	31°37′N, 88°59′E	KF691316–KF691318
6	57211	URM	42	U	U	Urmia Lake	Iran	45°28′E, 37°35′N	JX512748–JX512808
7	55582/1317	BAM	6	EHC	EHC	Bameng, Inner Mongolia	China	40°46′N, 107°27′E	KF691148–KF691153
8	64756/1233	CAN	4	EHC	EHC	Canghzhou, Hebei	China	38°32′N, 117°00′E	KF691166–KF691169
9	64767/1210	CHE	3	EHC	EHC	Chengkou, Shandong	China	117°43′E, 38°05′N	KF691170–KF691172
10	64762/1216	DON	3	EHC	EHC	Dongjiagou, Liaoning	China	121° 53′E, 39°04′N	KF691187–KF691189
11	64744/1199	GAH	6	EHC	EHC	Gahai, Qinghai	China	97°37′E, 37°07′N	KF691199–KF691204
12	65627/1211	HAN	7	EHC	EHC	Hangu, Tianjin	China	117°50′E, 39°25′N	KF691208–KF691214
13	64742/1077	SHA	3	EHC	EHC	Shanyao, Fuijan	China	118°53′E, 25°08′N	KF691233–KF691235
14	64764/1073	YIN	4	EHC	EHC	Yingkou, Liaoning	China	122°13′E, 40°40′N	KF691287–KF691290
15	65852	ELM	9	EHC	EHC	El Max Saline (Alexandria)	Egypt	31°08′N, 30°07′E	KP090303–KP090311
16	65851	ELA	6	EHC	EHC	Bourg El-Arab	Egypt	31°05′N, 30°03′E	KP090297–KP090302
17	65853	SAI	6	EHC	EHC	Port Saied	Egypt	31°25′N, 32°28′E	KP090312–KP090317
18	57227	INC	5	EHC	EHC	Incheh Lake, Gonbad, Golestan	Iran	37°24′N, 54°36′E	KF691333–KF691337
19	57223	LAGW	5	EHC	EHC	Lagoons around Urmia Lake, West Azerbaijan	Iran	37°15′N, 45°40′E	KF691338–KF691342
20	57224	LAGE	3	EHC	EHC	Lagoons around Urmia Lake, Dasht-E-Tabriz, East Azerbaijan	Iran	37°47′N, 45°25′E	KF691343–KF691345
21	57226	MIG	5	EHC	EHC	Mighan Salt Lake, Arak	Iran	34°20′N, 49°50′E	KF691357–KF691361
22	57225	QOM	6	EHC	EHC	Qom Salt Lake, Qom	Iran	34°40′N, 51°52′E	KF691367–KF691372
23	57255	ABG	3	EHC	EHC	Abu-Ghraib, Baghdad	Iraq	44°30′E, 33°20′N	KF691373–KF691375
24	57232	ARS	7	EHC	EHC	Aral Sea	Kazakhstan	45°52′N, 58°43′E	KF691391–KF691397
25	57233	ASS	6	EHC	EHC	Aral Sea (South)	Kazakhstan	44°43′N, 59°34′E	KF691398–KF691403
26	57235	KYZ	5	EHC	EHC	Kyzylkak	Kazakhstan	53°26′N, 73°48′E	KF691404–KF691408
27	57234	NCS	6	EHC	EHC	North Caspian sea	Kazakhstan	47°06′N, 51°55′E	KF691409–KF691414
28	57236	PAV	6	EHC	EHC	Pavlodar	Kazakhstan	52°18′N, 76°57′E	KF691415–KF691420
29	57231	TUZ	14	EHC	EHC	Tuz Lake, Pavlodar	Kazakhstan	51°19′N, 78°38′E	KF691421–KF691434
30	57295	ANK	7	EHC	EHC	Ankiembe saltworks	Madagascar	23°35′S, 43°60′E	KP090318–KP090324
31	57325/1720	BYA	5	EHC	EHC	Bolshoye Yarovoye, Altayskiy	Russia	52°50′N, 78°41′E	KF691455–KF691459
32	55586/1702	EBE	7	EHC	EHC	Ebeyty, Omskaya	Russia	54°59′N, 73°23′E	KF691460–KF691466
33	55581/1641	GOR	5	EHC	EHC	Gorkoye Lake	Russia	55°21′N, 68°32′E	KF691467–KF691471
34	64747/1389	KUC	3	EHC	EHC	Kuchukskoye, Altayskiy	Russia	52°42′N, 79°46′E	KF691472–KF691474
35	55579/1528	KUL	3	EHC	EHC	Kulundinskoye, Altayskiy	Russia	53°10′N, 79°30′E	KF691475–KF691477
36	64750/1640	KUR	4	EHC	EHC	Kurgan area	Russia	55°29′N, 64° 27′E	KF691478–KF691480
37	64752/1705	MME	4	EHC	EHC	Maloye Medvezhye (Kurganskaya)	Russia	55°12′N, 67°57′E	KF691481–KF691484
38	55585/1735	MYA	7	EHC	EHC	Maloye Yarovoye (Altayskiy)	Russia	53°4′N, 79°10′E	KF691485–KF691491
39	64749/1507	MED	3	EHC	EHC	Medvezhye (Kurganskaya)	Russia	66°4′E, 54°55′N	KF691492–KF691494
40	64751/1642	VOS	3	EHC	EHC	Voskresenskoye (Kurganskaya)	Russia	55°32′N, 67°23′E	KF691495–KF691497
41	57292/1512	CAM	10	EHC	U	Çamalti Saltern, Izmir	Turkey	26°53′E, 38°39′N	KF691520–KF691529
42	57258/1371	KBG	5	EHC	U	Kara Bogaz Gol	Turkmenistan	53°33′E, 41°17′N	KF691530–KF691534
43	57252/1715	CAA	9	EHC	EHC	Cape Aktymsyk, Karakalpakstan	Uzbekistan	43°54′N, 59°30′E	KF691547–KF691555

Samples are presented according to species designation and alphabetical order of country of origin. ARC, Laboratory of Aquaculture & *Artemia* Reference Centre, Ghent University, Belgium; IPMB, Institute of Pharmacy and Molecular Biotechnology, Heidelberg University, Germany. Putative species status: EHC, Eurasian haplotype complex; S, *A. sinica*; T, *A. tibetiana*; U, *A. urmiana*.

*A, species designation according to distribution; B, species designation according to haplotypes.

T = 0.33), nst = 6, rates = gamma, shape = 1.64, ncat = 4, pinvar = 0.53). An ML tree was reconstructed using MEGA 6 with all proposed parameters (Tamura *et al*., 2013). In our data set, the GTR model was used as a replacement for the suggested models because the suggested models were not implemented in MEGA 6.

Genetic distances [p-distances and Kimura two-parameter (K2P) nucleotide models] were calculated using MEGA 6. Population genetic diversity parameters, including haplotype diversity (HD), nucleotide diversity (π), number of polymorphic sites (V), and number of mutations (M) were calculated for each species using DnaSP 5.0 (Librado & Rozas, 2009). We performed two neutrality tests of Tajima's *D* (Tajima, 1989) and Fu's *Fs* (Fu, 1997) for each species, based on allele frequency, using ARLEQUIN 3.5 (Excoffier & Lischer, 2010) with a bootstrap of 10 000.

Interspecific genealogical relationships among *COI* haplotypes were reconstructed using median-joining network analysis, based on parsimony criteria (Bandelt, Forster & Rohl, 1999), implemented in the software NETWORK 4.6.1.0 (Forster, Bandelt & Röhl, 2004). The median joining algorithm with default settings was used for network construction (weight = 10; ε = 0). We constructed a *COI* haplotype map based on two criteria: (1) all individuals sequenced in IPMB; and (2) additional sequences from GenBank.

Analysis of molecular variance (AMOVA) was performed to find out genetic variation among the complete *COI* data set using ARLEQUIN 3.5 (Excoffier & Lischer, 2010) with 10 000 permutations. AMOVA was grouped based on species identified in the phylogenetic tree.

Molecular dating analysis

Bayesian analysis and divergence time estimation using BEAST

There are no fossil records in *Artemia*, and we therefore resorted to the secondary calibration of our clock models. Divergence time was set at 145 Mya, based on *Daphnia* O. F. Mueller, 1758 (Crustacea, Cladocera, Anomopoda), a fossil from the Jurassic/Cretaceous (Kotov & Taylor, 2011). The age of the most recent common ancestor (tMRCA) of all major clades is provided as a mean ± standard deviation.

Bayesian tree reconstruction and divergence times of Asian *Artemia* lineages were determined using BEAST 2.1.1.1 (Drummond & Rambaut, 2007) using the following parameters: nucleotide substitution model = GTR with four rate categories; gamma heterogeneity among species; molecular clock model = an uncorrelated lognormal relaxed model; and tree reconstruction = Birth–Death model. XML files for all BEAST runs were created using BEAUTi 1.7.4 (Drummond *et al*., 2012). The analysis was run twice independently for 40 million generations, taking samples every 1000 generations. Posterior probability distributions of parameters were obtained by Markov Chain Monte Carlo (MCMC) sampling. All runs were then combined after a burn-in of 10% using LogCombiner 1.7.2. TRACER 1.5 was used to verify the stationary distribution of acceptable mixing of the MCMC steps and to ensure that each parameter had been appropriately sampled (i.e. effective sampling size > 200). The maximum clade credibility tree using median heights was annotated using TreeAnnotator 1.7.2 and then inputted to FigTree 1.3.1 to visualize the tree and divergence times of lineages.

RESULTS

Genetic diversity and phylogenetic relationships

A total of 520 mitochondrial *COI* sequences were analysed for the whole data set present at IPMB and GenBank. The mitochondrial alignment consisted of an average of 560 nucleotides: 102 sites were polymorphic and 85 sites were parsimony informative. The maximum genetic distance was observed within *A. tibetiana* (2%) and the lowest was observed in *A. sinica* (0.5%). Pairwise genetic distances among *Artemia* lineages are summarized in Table 2.

The *COI* haplotype diversity within sexual Asian species was higher in *A. tibetiana* and *A. urmiana*, compared with putative asexual EHC lineages. The level of genetic diversity among EHC lineages was higher in Europe than in Asia or Africa (0.71 ± 0.05, 0.55 ± 0.03, and 0.41 ± 0.09, respectively). Statistics of sequence polymorphisms are detailed in Table 3, and the distribution of haplotypes for the *COI* data set within localities is shown in Tables S2 and S3.

Phylogenetic trees generated by ML and BI from *COI* sequences had concordant topologies, and found four distinct well-supported clades (Fig. 1), which

Table 2. Net nucleotide sequence divergence based on uncorrected p-distances (lower triangle) and Kimura two-parameter nucleotide models (K2P; upper triangle) for Asian *Artemia* species

Species	*A. sinica*	*A. tibetiana*	*A. urmiana*	EHC
A. sinica (24)*		0.158	0.179	0.172
A. tibetiana (36)	0.136		0.051	0.057
A. urmiana (72)	0.153	0.048		0.018
EHC (386)	0.148	0.052	0.018	

*Numbers in parenthesis indicates number of individuals examined per species.
1 = 100%.

Table 3. Genetic diversity indices for cytochrome *c* oxidase subunit I (*COI*) from *Artemia* species

Species	*N*	*V*	*M*	*H*	*HD*	π	*K*	Tajima's *D*	Fu's *F*u
A. sinica	24	7	7	6	0.7 ± 0.06	0.003 ± 0.002	1.38	−0.81	−1.01
A. tibetiana	36	42	42	17	0.9 ± 0.02	0.01 ± 0.006	10.68	0.197	−0.22
A. urmiana	79	48	49	34	0.88 ± 0.03	0.006 ± 0.005	3.40	−2.13*	−26.00**
EHC – Africa	38	9	9	7	0.41 ± 0.09	0.002 ± 0.001	1.22	−1.26	−1.65
EHC – Asia	283	48	49	22	0.55 ± 0.03	0.004 ± 0.003	2.11	−2.10*	−7.65**
EHC – Europe	58	24	24	13	0.71 ± 0.05	0.01 ± 0.003	7.25	1.27	2.20

N, sample size; *V*, number of polymorphic (segregating) sites; *M*, number of mutations; *H*, number of haplotypes; *HD*, haplotype diversity; π, nucleotide diversity; *K*, average number of pairwise differences.
Significance: ***$P < 0.001$; **$P < 0.01$; *$P < 0.05$.

correspond to the recognized *Artemia* species and the EHC complex. *Artemia sinica* clusters at the base of all Asian taxa; however, some specimens that were associated with EHC lineages in previous publications (Muñoz *et al*., 2010; Maniatsi *et al*., 2011; Maccari *et al*., 2013) cluster with *A. urmiana*, which would indicate that this species has a much wider distribution than was previously assumed.

A *COI* phylogeny network from IPMB sequences showed 45 distinct haplotypes that are connected together with a maximum number of 105 mutational steps (Fig. 2). EHC lineages consisted of two major haplotypes (H1 and H3), from which other haplotypes derive with frequencies between five and seven. Numerous singleton haplotypes surrounded the major haplotypes. Haplotypes did delineate a genetic partition corresponding to species designation, except for H19 and H28. These two haplotypes showed up in Lake Urmia, Iran, and had therefore been considered as *A. urmiana* by Eimanifar & Wink (2013), but according to this analysis they belong to the EHC complex. *Artemia urmiana* lineages consisted of two major haplotypes (H5 and H15) with multiple singleton haplotypes.

The *COI* haplotype network of the complete data set (IPMB + GenBank) showed a more complex architecture, comprising 69 different haplotypes, 118 mutational steps, and four major haplotypes that were exclusive to the major species of *Artemia* (Fig. 3). The EHC lineages revealed a typical star-like topology and a short genealogy. The central haplotype H3 was the most abundant (44%, or 228 out of 520 individuals), including individuals from Eurasia and Africa. Haplotype H52 consisted of individuals from Tibet (China) that were considered *A. tibetiana* by Maccari *et al*. (2013), but according to this analysis are part of EHC.

Artemia urmiana consists of a haplotype complex including two major haplotypes (H5 and H37), surrounded by several haplotypes with frequencies between two and seven. Haplotypes H2, H5, H7, H19, H46, H47, H48, and H50 correspond to individuals from Bulgaria, China, Greece, Ukraine, Tibet (China), Turkey, and Turkmenistan, indicating that *A. urmiana* has a wide distribution and comprises haplotypes that had been regarded as belonging to the EHC complex.

Artemia sinica is represented by two major haplotypes (H30 and H32) with a strong geographical structure in Asia. *Artemia tibetiana* showed one major haplotype (H21) and several other haplotypes that have a close genetic relationship with *A. urmiana* and EHC.

The AMOVA analysis indicated that most of the genetic variation was partitioned between lineages (94%, $P < 0.05$), whereas 6% of genetic variation was attributed within each species of *Artemia*. The average genetic differentiation index (F_{ST}) for all lineages was calculated to be 0.94.

Estimation of divergence times

According to the *COI* tree rooted with *Daphnia* the divergence between *A. sinica* and other Asian species took place in the late Miocene, *c*. 19.99 Mya (9.37–36.69 Mya). The split between *A. tibetiana* and *A. urmiana* + EHC clades occurred in the late Pliocene, *c*. 5.41 Mya (2.19–9.99 Mya) (Fig. 4). The split between *A. urmiana* and EHC clades happened in the Pleistocene, *c*. 2.03 Mya (0.75–3.54 Mya). According to our calibration, diversification within *A. urmiana* and EHC lineages took place in the Pleistocene and Holocene (Fig. 4).

DISCUSSION

Asian *Artemia* phylogeography and haplotype network

By combining the existing information from previous studies, with that of the present multispecies study we were able to unravel the phylogeographic structure and evolutionary history of Asian *Artemia*. Our *COI* phylogeny based on ML and BI approaches determined that Asian lineages cluster into four clades. Sexual species have a pronounced genetic structure and are geographically isolated, with the exception of

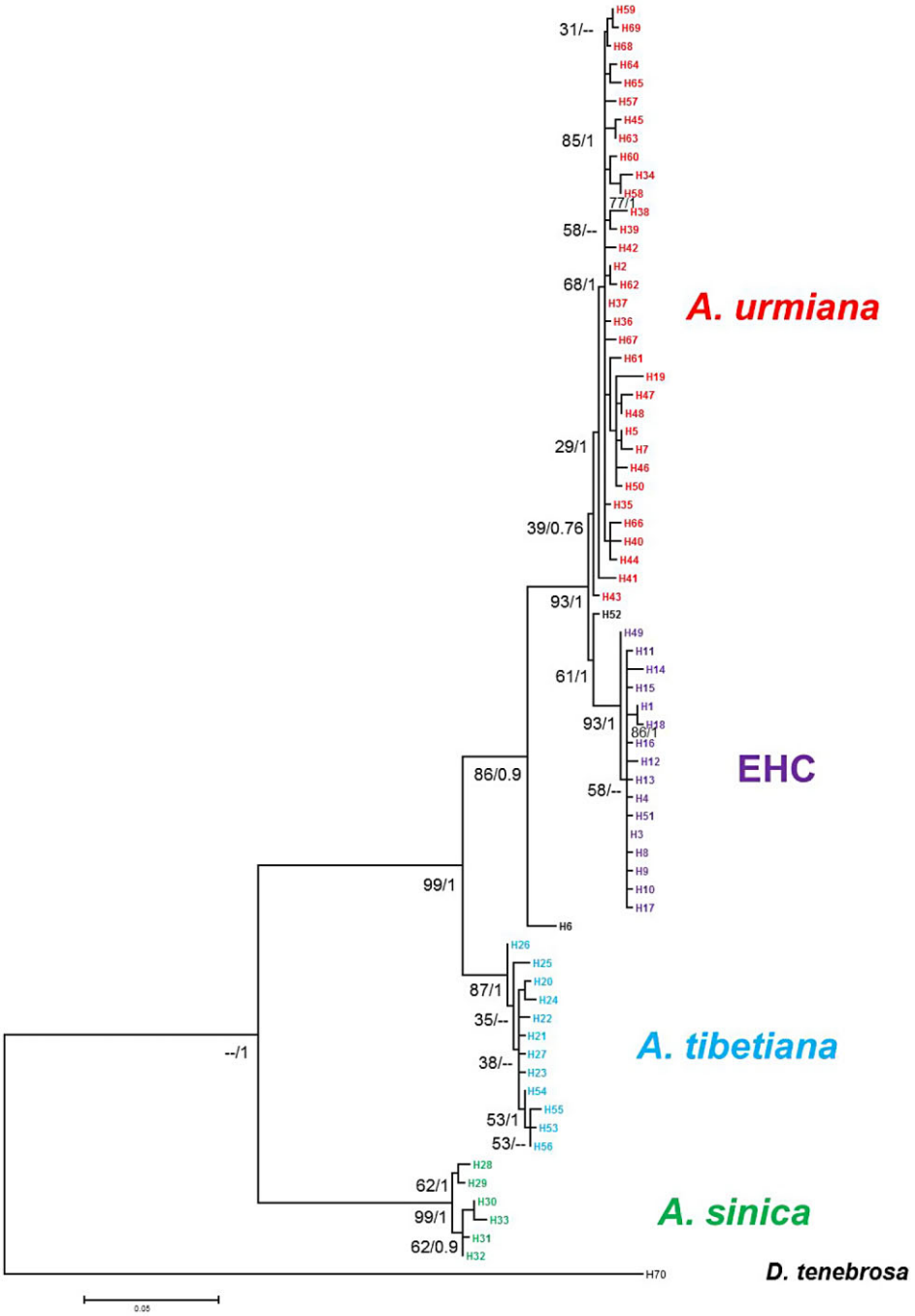

Figure 1. Maximum-likelihood (ML) phylogram for 70 unique haplotypes of Asian *Artemia* based on the cytochrome *c* oxidase subunit I (*COI*) marker. The ML bootstrap values and Bayesian supports are shown for each major node, from left to right. Haplotypes found for each species correspond to associated individuals listed in Table S3. Each species is illustrated with different colours. The tree is rooted with *Daphnia tenebrosa* (H70) as an out-group.

A. urmiana, which shows a much wider distribution outside Urmia Lake than was previously assumed. The putative parthenogenetic EHC lineages showed a narrow genetic structure and are widely distributed across Eurasia (Lázaro *et al.*, 2009; Maccari *et al.*, 2013).

The interspecific sequence divergence based on p-distances varied between 1.8 and 15.3%. The *COI* interspecific values are within the range reported for other aquatic crustaceans, such as: Anostraca, the fairy shrimp (0.012–0.058%; Reniers *et al.*, 2013); Daphina

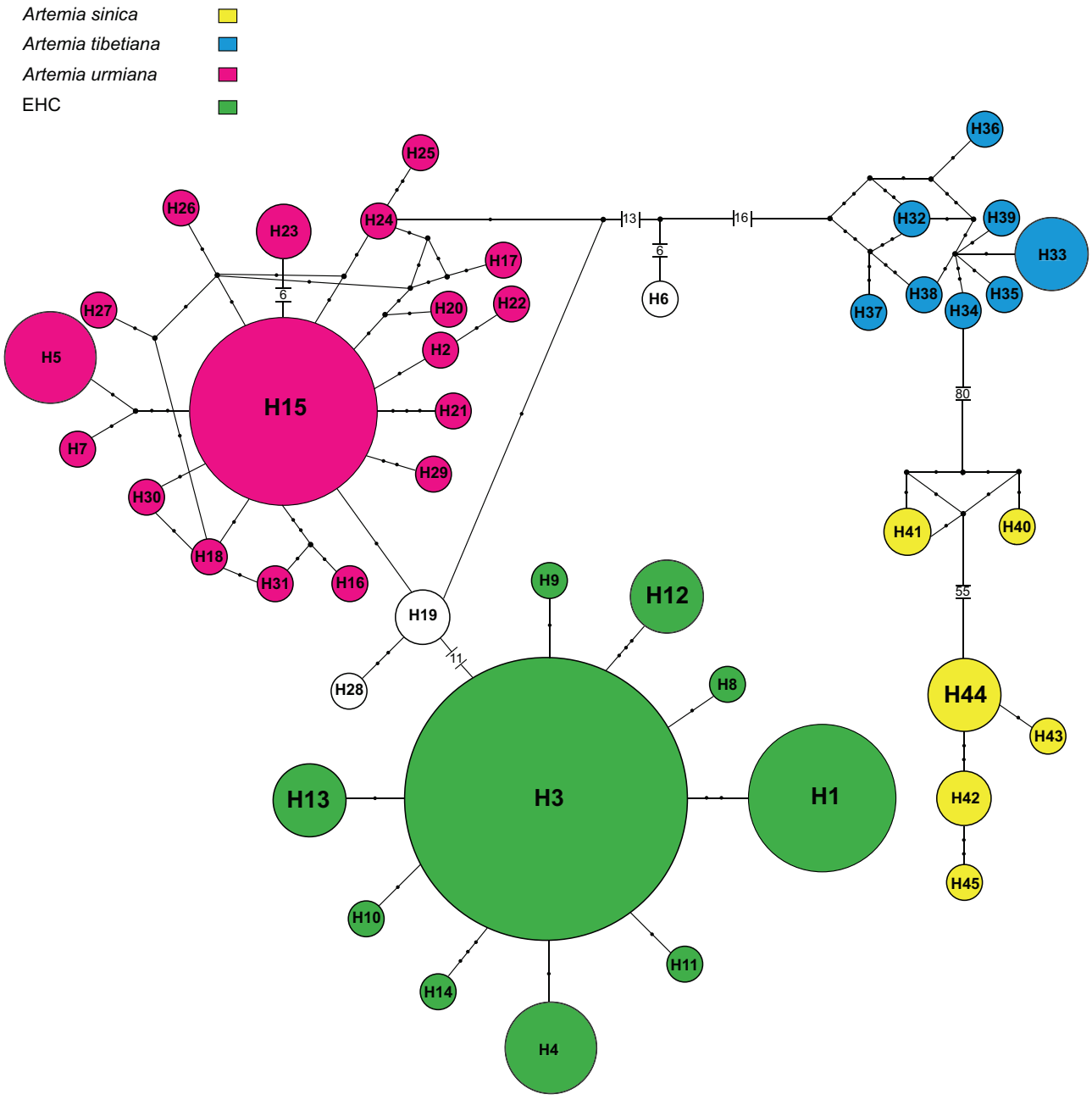

Figure 2. The cytochrome *c* oxidase subunit I (*COI*) haplotype network for Asian *Artemia* lineages (IPMB sequences), reconstructed by statistical parsimony. Haplotype frequencies are proportional to circle size. Circles are coloured according to species description. A small black circle indicates the number of mutational steps separating haplotypes. Associated individuals with their frequencies for each haplotype are listed in Table S2.

(2.6–5.7%; Hebert, Witt & Adamowicz, 2003); rotifers (0.2–13.1%); and decapods (0.28–1.37%).

A peculiarity in the *COI* haplotype network is the observation that some individuals corresponding to haplotypes H2, H5, H7, H19, H46, H47, H48, and H50, which had been considered to be part of the EHC group (Muñoz *et al*., 2010; Maniatsi *et al*., 2011; Maccari *et al*., 2013; Eimanifar *et al*., 2014), cluster within *A. urmiana*. According to our network, there are four hypotheses to explain this condition. Firstly, some samples were wrongly assumed as belonging to parthenogenetic lineages, and morphological differences hardly exist between *Artemia* taxa. Secondly, EHC lineages show a recent origin, as they might have originated from

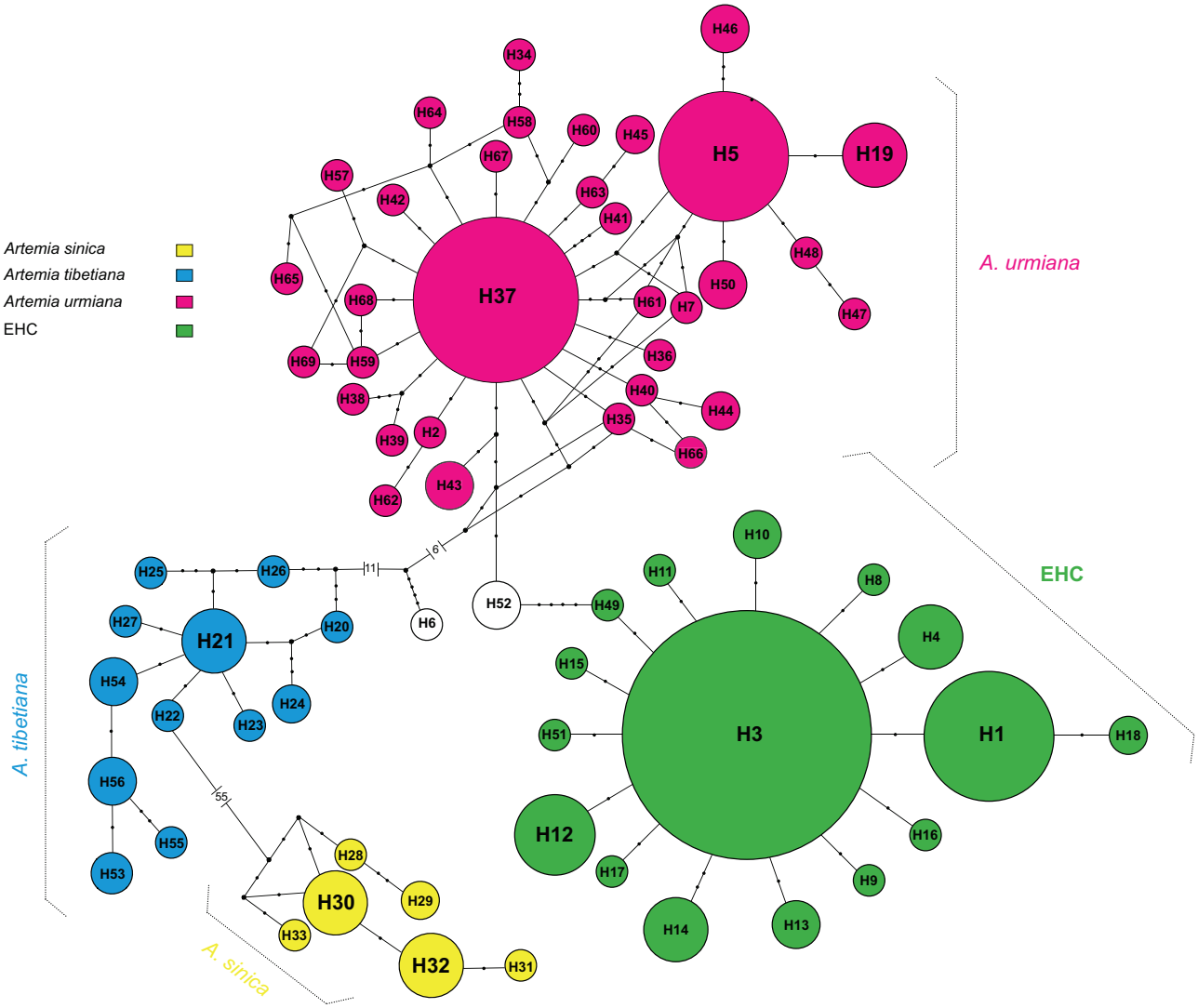

Figure 3. Median-joining network of cytochrome *c* oxidase subunit I (*COI*) haplotypes of *Artemia* (IPMB and GenBank sequences). Each circle corresponds to haplotypes exhibiting the number of individuals. Circles are coloured according to species description. A small black circle indicates the number of mutational steps separating haplotypes. Associated individuals with their frequencies for each haplotypes are listed in Table S3.

Asian sexual species (Baxevanis *et al*., 2006; Muñoz *et al*., 2010; Maccari *et al*., 2013). Assuming that they have recently expanded, some individuals would not have had sufficient time to diverge from their original sexual species (Law & Crespi, 2002). Thirdly, *A. urmiana* might have dispersed to adjacent regions via migratory birds or human activities, so that this taxon is no longer endemic in Asia (Abatzopoulos *et al*., 2009). The latter hypothesis needs to be carefully reassessed, as we only deal with mtDNA sequence variation and thus more detailed systematic investigations using ncDNA markers and life-history studies are required for the populations studied so far, or for other unexplored localities in Eurasia and Africa. Fourthly, three haplotypes, H19, H28, and H52, which had been considered to represent *A. urmiana* and *A. tibetiana*, according to their geographic distribution, are apparently members of EHC (Figs 2, 3). Whether this discrepancy arises from hybridization between EHC lineages and sexual species in Asia (Baxevanis *et al*., 2006) or just from erroneously identified samples, should be analysed.

Genetic diversity of EHC

The EHC exhibited an overall lower genetic diversity and a shallow structure, resulting from recent evolutionary expansion (Muñoz *et al*., 2010); however,

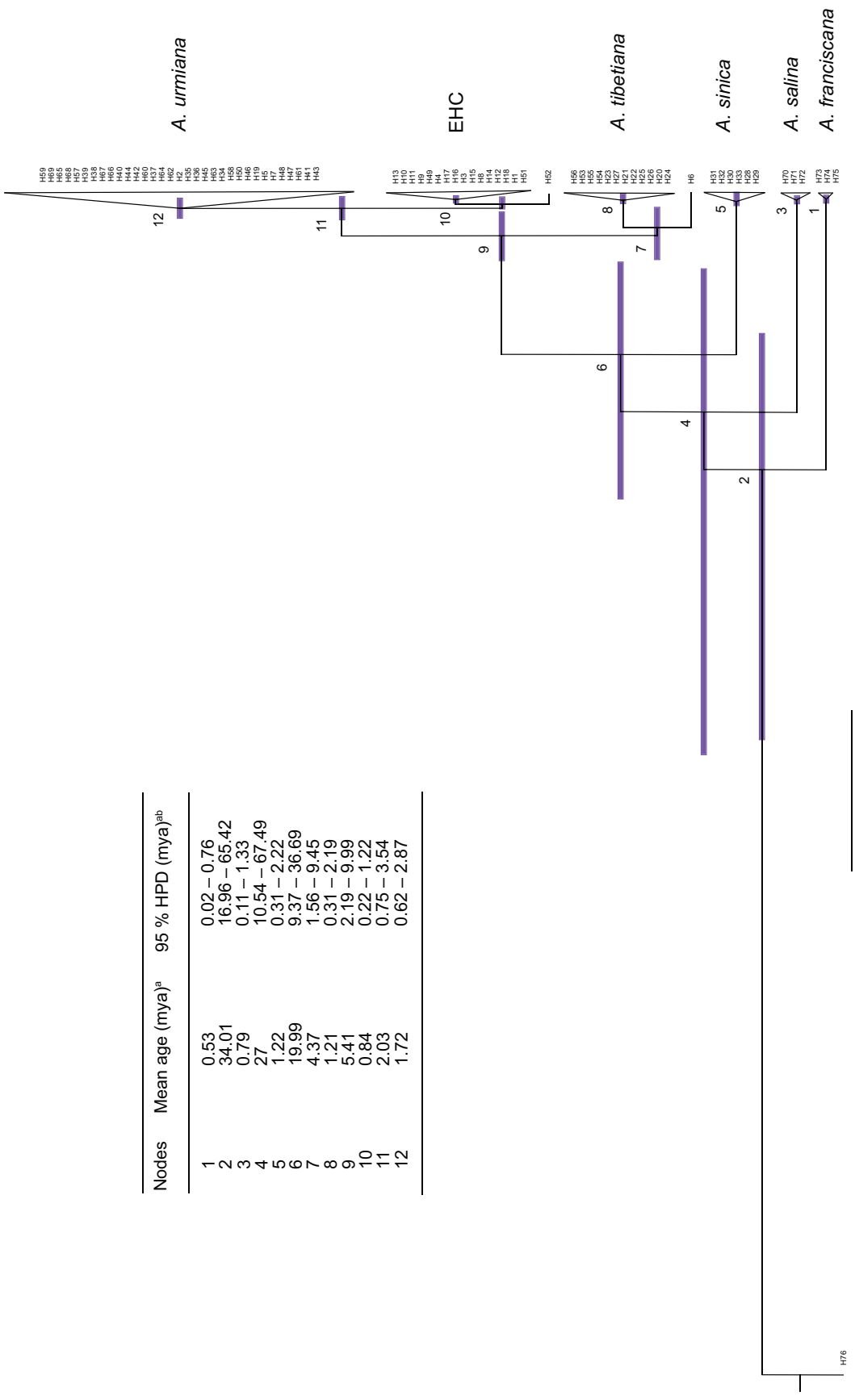

Nodes	Mean age (mya)[a]	95 % HPD (mya)[ab]
1	0.53	0.02 – 0.76
2	34.01	16.96 – 65.42
3	0.79	0.11 – 1.33
4	27	10.54 – 67.49
5	1.22	0.31 – 2.22
6	19.99	9.37 – 36.69
7	4.37	1.56 – 9.45
8	1.21	0.31 – 2.19
9	5.41	2.19 – 9.99
10	0.84	0.22 – 1.22
11	2.03	0.75 – 3.54
12	1.72	0.62 – 2.87

Figure 4. A chronogram for the Asian *Artemia* lineages obtained under a relaxed clock model using cytochrome *c* oxidase subunit I (*COI*). The blue node bars indicate 95% posterior probability intervals. The geological timescale is in Myr. The mean divergence times for major nodes is shown by numbers. Each number corresponds to divergence times listed in the table. The tree is externally calibrated with fossil evidence. [a]mya, million years ago; [ab]refers to lower and upper 95% highest posterior density (HPD) intervals.

European EHC lineages revealed a higher genetic diversity as compared with those from Asia and Africa. Possible explanations are firstly the fact that environmental heterogeneities, such as in climate and in hydrology, could influence extinction or colonization processes, shaping genetic variation among lineages (Storfer *et al.*, 2010; Maccari *et al.*, 2013). Secondly, high frequencies of mutation and possibly the presence of rare males in parthenogenetic European/African EHC lineages could enhance genetic diversity (Simon *et al.*, 2003; Lo, Stefanovic & Dickinson, 2009; Maccari *et al.*, 2013, 2014). Contagious parthenogenesis has important evolutionary consequences at it results in the repeated generation of new asexual genotypes, increasing the genetic diversity in parthenogens. This counteracts the loss of asexual genotypes resulting from the accumulation of deleterious mutations (Muller's ratchet) of gene conversion (Tucker *et al.*, 2013), and could contribute to the evolutionary success of parthenogenesis (Simon *et al.*, 2003).

Divergence times between sexual/asexual Asian lineages

The dates of divergence among *Artemia* species are controversial. This is because of the absence of fossil evidence in this genus. Our study is based on a secondary calibration with a *Daphnia* fossil, the evolutionary age of which is known. Based on our *COI* information, New and Old World *Artemia* shared a common ancestor about 34 Mya, whereas the divergence within Asian lineages started about 20 Mya in the late Miocene, which is partially in accordance with other estimates based on nuclear genes (Baxevanis *et al.*, 2006). All EHC lineages and *A. urmiana* shared a common ancestor around 2.03 Mya (Pleistocene). EHC lineages are young, with a diversification within the last 0.84 Myr (Holocene).

Geological data indicate that the Qinghai–Tibet Plateau is a relatively young region formed by extensive India–Eurasia tectonic activity in the early Tertiary, between 45 and 50 Mya (Molnar, 2005). Hydrochemical and palaeoclimatological characteristics of the Tibet Plateau have resulted in the adaptation of *A. tibetiana* in a novel ecological region (Abatzopoulos *et al.*, 2002; Zhang *et al.*, 2013). In our study, *A. tibetiana* revealed a recent diversification in the early Pleistocene, roughly 1.21 Mya, which is mostly associated with the young geological age of different smaller saline lakes in Tibet, ranging from the Eocene to the Pleistocene (Zheng, 1997; Eimanifar *et al.*, 2014). The Tibet Plateau has been uplifted, according to geological and thermochronological evidence, which has eventually caused a semi-complete geographic separation between western (*A. urmiana*) and eastern (*A. sinica*) bisexual *Artemia* species (Van Stappen, 2008; Wang *et al.*, 2012). North-eastern China is a geographical region inhabited by *A. sinica*. The eastern part of Tibet has undergone rapid elevation between 9 and 13 Mya, which coincides with the divergence time of *A. sinica* from the rest of the Asian populations (Clark *et al.*, 2005).

Based on biogeographical evidence, Baxevanis *et al.* (2006) assumed that EHC lineages diverged from *A. urmiana* 11 Mya, and that *A. sinica* diverged from the other Asian species *c.* 8 Mya. The divergence time within EHC lineages was assumed to be 3.5 Mya. As discussed before, our DNA data implicate a much more recent time scenario. Muñoz *et al.* (2010) emphasized that EHC lineages from Africa and Europe are relatively young, and are related to Holocene refugia. Manaffar *et al.* (2011) have argued that *A. urmiana* diverged 11 Mya, whereas Urmia Lake appears to have been formed later than that, in the late Pleistocene. If these estimates are correct, *A. urmiana* must have originated elsewhere and was later dispersed to Urmia Lake. Shadrin, Anufriieva & Galagovets (2012) supported this hypothesis because *Artemia* cysts extracted from sediment cores of Urmia Lake were roughly 5000 years old and most likely parthenogenetic. It was suggested that *A. urmiana* might have originated in the Miocene in Crimean salt lakes (Shadrin *et al.*, 2012; Anufriieva & Shadrin, 2013); however, this hypothesis looks speculative as no *Artemia* fossils have yet been found.

In conclusion, our phylogeographic analysis revealed the presence of multiple *COI* haplotypes in Eurasia that can be grouped into four major lineages. Thus more than one haplotype is present in most Asian salt lakes. The question remains whether the brine shrimps with distinctive haplotypes represent distinct species (as assumed in most publications). Do barriers exist that prevent hybridization when they live in the same lake? Or do some local populations represent hybridizing species complexes? More sequence data, especially from nuclear genes and other biparental markers (e.g. microsatellite data) are needed to better understand the evolution and biology of *Artemia*.

ACKNOWLEDGEMENTS

A.E. was supported by a PhD fellowship from the Deutscher Akademischer Austauschdienst (DAAD, German Academic Exchange Service). We thank Prof. Gonzalo Gajardo (Laboratorio de Genética, Acuicultura & Biodiversidad, Universidad de Los Lagos, Osorno, Chile) for his reading and useful comments on this article. We would like to express our appreciation to Prof. Li Sanzhong (Department of Marine Geosciences, Ocean University of China, Qingdao, China) for his generous comments and explanation of geological events in Asia.

REFERENCES

Abatzopoulos TJ, Amat F, Baxevanis AD, Belmonte G, Hontoria F, Maniatsi S, Moscatello S, Mura G, Shadrin N. 2009. Updating geographic distribution of *Artemia urmiana* Günther, 1890 (Branchiopoda: Anostraca) in Europe: an integrated and interdisciplinary approach. *International Review of Hydrobiology* **94:** 560–579.

Abatzopoulos TJ, Beardmore JA, Clegg JS, Sorgeloos P. 2002. Artemia*: basic and applied biology*. Dordrecht, The Netherlands: Kluwer Academic Publishers.

Abatzopoulos TJ, Zhang B, Sorgeloos P. 1998. *Artemia tibetiana*: preliminarycharacterization of a new *Artemia* species found in Tibet (People's Republic of China). International study on *Artemia* LIX. *International Journal of Salt Lake Research* **7:** 41–44.

Anufriieva E, Shadrin N. 2013. Hypothesis of the origin of *Artemia urmiana* (Anostraca, Crustacea) in the Crimea: an essay of the paleo-reconstruction. *Scientific Notes of Taurida National University named after VI Vernadsky: Geography* **26:** 3–8. (in Russian).

Bandelt HJ, Forster P, Rohl A. 1999. Median-joining networks for inferring intraspecific phylogenies. *Molecular Biology and Evolution* **16:** 37–48.

Barigozzi C. 1974. *Artemia*: a survey of its significance in genetic problems. In: Dobzhansky T, Hecht MK, Steere WC, eds. *Evolutionary biology*. New York: Springer, 221–252.

Baxevanis AD, Kappas I, Abatzopoulos TJ. 2006. Molecular phylogenetics and asexuality in the brine shrimp *Artemia*. *Molecular Phylogenetics and Evolution* **40:** 724–738.

Cai Y. 1989. A redescription of the brine shrimp (*Artemia sinica*). *The Wasmann Journal of Biology* **47:** 105–110.

Clark MK, House MA, Royden LH, Whipple KX, Burchfiel BC, Zhang X, Tang W. 2005. Late cenozoic uplift of southeastern Tibet. *Geology* **33:** 525–528.

Drummond AJ, Rambaut A. 2007. BEAST: Bayesian evolutionary analysis by sampling trees. *BMC Evolutionary Biology* **7:** 214.

Drummond AJ, Suchard MA, Xie D, Rambaut A. 2012. Bayesian phylogenetics with BEAUti and the BEAST 1.7. *Molecular Biology and Evolution* **29:** 1969–1973.

Eimanifar A, Van Stappen G, Marden B, Wink M. 2014. *Artemia* biodiversity in Asia – phylogeography of the introduced American species *Artemia franciscana* Kellogg, 1906. *Molecular Phylogenetics and Evolution* **79:** 392–403.

Eimanifar A, Wink M. 2013. Fine-scale population genetic structure in *Artemia urmiana* (Günther, 1890) based on mtDNA sequences and ISSR genomic fingerprinting. *Organisms, Diversity and Evolution* **13:** 531–543.

Excoffier L, Lischer HEL. 2010. Arlequin suite ver 3.5: a new series of programs to perform population genetics analyses under Linux and Windows. *Molecular Ecology Resources* **10:** 564–567.

Forster P, Bandelt HJ, Röhl A. 2004. Network 4.2.0.1. Fluxus Technology Ltda. Software free. Available at: http://www.fluxus-engineering.com/sharenet.htm

Fu YX. 1997. Statistical tests of neutrality of mutations against population growth, hitchhiking and background selection. *Genetics* **147:** 915–925.

Gajardo GM, Beardmore JA. 2012. The brine shrimp *Artemia*: adapted to critical life conditions. *Frontiers in Physiology* **3:** 185.

Günther RT. 1899. Contributions to the natural history of Lake Urmia, N.W Persia, and its neighbourhood. *Zoological Journal of the Linnean Society* **27:** 345–453.

Hall TA. 1999. BioEdit: a user-friendly biological sequence alignment editor and analysis program for windows 95/98/NT. *Nucleic Acids Symposium Series* **41:** 95–98.

Hebert PD, Witt JD, Adamowicz SJ. 2003. Phylogeographical patterning in *Daphnia ambigua*: regional divergence and intercontinental cohesion. *Limnology and Oceanography* **48:** 261–268.

Kotov AA, Taylor DJ. 2011. Mesozoic fossils (> 145 mya) suggest the antiquity of the subgenera of *Daphnia* and their coevolution with chaoborid predators. *BMC Evolutionary Biology* **11:** 129.

Law JH, Crespi BJ. 2002. The evolution of geographic parthenogenesis in Timema walking-sticks. *Molecular Ecology* **11:** 1471–1489.

Lázaro EM, Sluys R, Pala M, Stocchino GA, Baguñà J, Riutort M. 2009. Molecular barcoding and phylogeography of sexual and asexual freshwater planarians of the genus Dugesia in the Western Mediterranean (Platyhelminthes, Tricladida, Dugesiidae). *Molecular Phylogenetics and Evolution* **52:** 835–845.

Librado P, Rozas J. 2009. DnaSP v5: a software for comprehensive analysis of DNA polymorphism data. *Bioinformatics* **25:** 1451–1452.

Lo EY, Stefanovic S, Dickinson TA. 2009. Population genetic structure of diploid sexual and polyploid apomictic hawthorns (Crataegus; Rosaceae) in the Pacific Northwest. *Molecular Ecology* **18:** 1145–1160.

Maccari M, Amat F, Gómez A. 2013. Origin and genetic diversity of diploid parthenogenetic *Artemia* in Eurasia. *PLoS ONE* **8:** e83348.

Maccari M, Amat F, Hontoria F, Gómez A. 2014. Laboratory generation of new *Artemia* parthenogenetic lineages through contagious parthenogenesis. *PeerJ* **2:** e333v1.

Manaffar R, Zare S, Agh N, Siyabgodsi A, Soltanian S, Mees F, Van Stappen G. 2011. Sediment cores from Lake Urmia (Iran) suggest the inhabitation by parthenogenetic *Artemia* around 5,000 years ago. *Hydrobiologia* **671:** 65–74.

Maniatsi S, Baxevanis AD, Kappas I, Deligiannidis P, Triantafyllidis A, Papakostas S, Bougiouklis D, Abatzopoulos TJ. 2011. Is polyploidy a persevering accident or an adaptive evolutionary pattern? The case of the brine shrimp *Artemia*. *Molecular Phylogenetics and Evolution* **58:** 353–364.

Molnar P. 2005. Mio-Pliocene growth of the Tibetan plateau and evolution of East Asian climate. *Palaeontologica Electronica* **8:** 1–23.

Muñoz J, Gómez A, Green AJ, Figuerola J, Amat F, Rico C. 2010. Evolutionaryorigin and phylogeography of the diploid

obligate parthenogen *Artemia parthenogenetica* (Branchiopoda: Anostraca). *PLoS ONE* **5:** 1–9.

Pilla EJS, Beardmore JA. 1994. Genetic and morphometric differentiation in Old World bisexual species of *Artemia* (the brine shrimp). *Heredity* **73:** 47–56.

Posada D. 2008. jModelTest: phylogenetic model averaging. *Molecular Biology and Evolution* **25:** 1253–1256.

Reniers J, Vanschoenwinkel B, Rabet N, Brendonck L. 2013. Mitochondrial gene trees support persistence of cold tolerant fairy shrimp throughout the Pleistocene glaciations in both southern and more northerly refugia. *Hydrobiologia* **714:** 155–167.

Shadrin N, Anufriieva E, Galagovets E. 2012. Distribution and historical biogeography of *Artemia* leach, 1819 (Crustacea: Anostraca) in Ukraine. *International Journal of Artemia Biology* **2:** 30–42.

Simon JC, Delmotte F, Rispe C, Crease T. 2003. Phylogenetic relationships between parthenogens and their sexual relatives: the possible routes to parthenogenesis in animals. *Biological Journal of the Linnean Society* **79:** 151–163.

Storfer A, Murphy MA, Spear SF, Holderegger R, Waits LP. 2010. Landscape genetics: where are we now? *Molecular Ecology* **19:** 3496–3514.

Tajima F. 1989. Statistical methods to test for nucleotide mutation hypothesis by DNA polymorphism. *Genetics* **123:** 585–595.

Tamura K, Stecher G, Peterson D, Filipski A, Kumar S. 2013. MEGA6: molecular evolutionary genetics analysis version 6.0. *Molecular Biology and Evolution* **30:** 2725–2729.

Tucker AE, Ackerman MS, Eads BD, Xu S, Lynch M. 2013. Population-genomic insights into the evolutionary origin and fate of obligately asexual *Daphnia pulex*. *Proceedings of the National Academy of Sciences of the United States of America* **110:** 15740–15745.

Van Stappen G. 2008. *Artemia* biodiversity in Central and Eastern Asia. PhD thesis, Ghent University, Belgium. Pp 1–132.

Wang Y, Zheng J, Zhang W, Li S, Liu X, Yang X, Liu Y. 2012. Cenozoic uplift of the Tibetan Plateau: evidence from the tectonic–sedimentary evolution of the western Qaidam basin. *Geoscience Frontiers* **3:** 175–187.

Xu S, Innes DJ, Lynch M, Cristescu ME. 2013. The role of hybridization in the origin and spread of asexuality in *Daphnia*. *Molecular Ecology* **22:** 4549–4561.

Zhang H, Luo Q, Sun J, Liu F, Wu G, Yu J, Wang W. 2013. Mitochondrial genome sequences of *Artemia tibetiana* and *Artemia urmiana:* assessing molecular changes for high plateau adaptation. *Science China Life Sciences* **56:** 440–452.

Zheng M. 1997. *An introduction to saline lakes on the Qinghai-Tibet Plateau*. Dordrecht, the Netherlands: Kluwer Academic Publishers.

SUPPORTING INFORMATION

Additional supporting information may be found in the online version of this article at the publisher's web-site:

Table S1. List of *Artemia* GenBank sample accession numbers used in *COI* phylogenetic analysis.
Table S2. Data matrix of variable sites and distribution of unique haplotypes with their frequencies among 243 *Artemia* individuals using 560 nt of *COI*.
Table S3. Data matrix of variable sites and distribution of unique haplotypes with their frequencies among 520 *Artemia* individuals using 560 nt of *COI*.